KERNFORSCHUNGSZENTRUM

KARLSRUHE

June 1970

KFK 1231
IAEA-CN-26/11

Institut für Angewandte Kernphysik

High Resolution Measurements of Radiative Neutron Capture in ^{47}Ti, ^{56}Fe, ^{58}Ni, ^{60}Ni and ^{61}Ni between 7 and 200 keV

A. Ernst, F.H. Fröhner, D. Kompe

GESELLSCHAFT FUR KERNFORSCHUNG M.B.H.

KARLSRUHE

KERNFORSCHUNGSZENTRUM KARLSRUHE

June 1970

KFK 1231
IAEA-CN-26/11

Institut für Angewandte Kernphysik

High Resolution Measurements of Radiative Neutron Capture in ^{47}Ti, ^{56}Fe, ^{58}Ni, ^{60}Ni and ^{61}Ni between 7 and 200 keV*

A. Ernst**, F.H. Fröhner, D. Kompe***

* Paper presented at the Second International Conference on Nuclear Data for Reactors, Helsinki, June 15 - 19, 1970.

** Associated with the University of Vienna, Austria.

*** Present address: Philips Elektrologica, 5904 Eiserfeld, West Germany.

Gesellschaft für Kernforschung mbH., Karlsruhe

ABSTRACT

Neutron capture in enriched samples of ^{47}Ti, ^{56}Fe, ^{58}Ni, ^{60}Ni and ^{61}Ni has been measured in the energy range 7 - 200 keV with the time-of-flight method. The time resolution was better than 2 ns/m. Neutrons were produced by a pulsed 3 MV Van de Graaff accelerator via the $Li^{7}(p,n)$ reaction. Capture events were detected with an 800 l liquid scintillator tank. The $^{197}Au(n,\gamma)$ cross section served as standard. Incorporation of transmission results, especially of resonance spins and total widths, in the analysis and careful treatment of multiple scattering permitted the determination of radiation widths for a large number of s-wave resonances.

ZUSAMMENFASSUNG

Neutroneneinfang in angereicherten Proben von ^{47}Ti, ^{56}Fe, ^{58}Ni, ^{60}Ni und ^{61}Ni wurde im Energiebereich 7 - 200 keV mittels der Flugzeitmethode gemessen. Die Zeitauflösung war besser als 2 ns/m. Neutronen wurden an einem gepulsten 3 MeV-Van-de-Graaff-Beschleuniger mit Hilfe der $Li^{7}(p,n)$-Reaktion erzeugt. Ein Flüssigszintillatortank von 800 l Inhalt diente zum Nachweis der Einfangereignisse. Der ^{197}Au (n,γ)-Querschnitt wurde als Standard benutzt. Durch Einbeziehung von Transmissionsergebnissen, insbesondere von Resonanzspins und Gesamtbreiten, in die Auswertung sowie durch sorgfältige Behandlung der Vielfachstreuung gelang es, die Strahlungsbreiten einer großen Zahl von s-Wellen-Resonanzen zu ermitteln.

1. INTRODUCTION

High resolution measurements of radiative neutron capture in the keV region are of interest to the designers of fast reactors, to nuclear structure physicists and to astrophysicists. The measurements described here are part of a programme to investigate structural materials for fast reactors.

2. EXPERIMENTAL APPARATUS

Capture yield versus neutron energy was measured using the time-of-flight method. 1 ns neutron pulses with a broad energy spectrum were produced with a repetition frequency of 500 kc/s by the $^{7}Li(p,n)^{7}Be$ reaction with protons from a pulsed 3 MV Van de Graaff accelerator. Samples were exposed to the well-collimated neutron beam in a cylindrical hole at the center of a 1.1 m liquid scintillator tank at a distance of 2 m from the target. The sample to be analyzed was interchanged at short time intervals with a carbon sample, which served to determine the time-dependent background, and with a gold sample, which was used to determine the neutron flux (ref. [1]). All signals from the detector exceeding a bias equivalent to 3 MeV were sorted by an on-line computer into a three-dimensional spectrum according to the time-of-flight, the total gamma ray energy absorbed in the scintillator and the number of the sample. This enabled us to obtain crude gamma ray spectra for individual resonances. Gamma ray spectra averaged over many resonances were also recorded separately down to 0.5 MeV pulse height. The scintillator tank described in ref. [2] was optically separated into four parts to allow majority coincidence operation in an attempt to get qualitative information on gamma ray multiplicities for individual resonances.

3. EXPERIMENTAL METHOD

Because the storage space of the on-line computer was insufficient to cover the whole energy region, there were two experimental runs for each isotope: a low energy run and a high energy run. In the low energy run, capture yields in the energy range from 6 to 11 keV were measured with 4 ns per channel, from 11 to 43 keV with 2 ns per channel and from 43 keV upwards with 16 ns per channel with a maximum neutron energy of 70 keV. In the high energy run, capture yields from 6 to 19 keV were measured with 8 ns per channel and from 19 keV upwards with 2 ns per channel with a maximum neutron energy between 160 and 230 keV, depending on the isotope. A typical experimental run took about 3 days. Every 12 hours, data were read out and time and energy calibrations were established to check the stability of the electronics. Each isotope was also measured down to 1 keV neutron energy in order to determine the possible overlap of neutrons from one pulse of the accelerator with low energy neutrons from the preceeding pulse of the accelerator. Only in the case of ^{47}Ti a correction had to be applied to the data due to neutron capture in a resonance at 3 keV.

4. SAMPLES

All samples to be analyzed were powders pressed into flat cylindrical bronze containers with a diameter of 8 cm. Carbon samples were graphite discs with thicknesses chosen to match the scattering cross section of the sample to be analyzed. They were placed into the same type of container. The gold sample was a disc 1 mm thick. The sample characteristics are listed in Table I.

5. ANALYSIS

From a three-dimensional spectrum obtained during one experimental run pulse height spectra for all samples were extracted covering the gamma energy range from 3 MeV to well above the neutron binding energy. These pulse height spectra were extrapolated to zero gamma ray energy with the aid of the average pulse height spectrum shapes obtained from the separately recorded pulse height data going down to 0.5 MeV gamma ray energy. The pulse height channels to be included in the capture-yield analysis were determined by a separate calculation in order to get a minimum for the combined statistical and systematic error in the capture yield. Then the time-of-flight spectra contained in these pulse height channels were added and the spectrum fraction contained in the resulting time-of-flight spectrum was calculated. In another calculation, the average neutron energy for each channel was computed from the flight path, from the position of the accelerator gamma flash (corrected for the photon flight time) and from the channel widths obtained from the time calibration data. Nonlinearities in the time-to-digital conversion electronics were taken into account. From all these data the capture yield divided by the sample thickness was calculated for each time-of-flight channel by the formula

$$"\sigma_\gamma" = \frac{(C_X - C_{SX}) \cdot N_A \cdot \varepsilon_A}{(C_A - C_{SA}) \cdot N_X \cdot \varepsilon_X} \sigma_{\gamma A}$$

where C_X denotes the counting rate for the analyzed sample, C_{SX} the counting rate for the carbon sample, obtained by adding up the same pulse height channels as in the case of the analyzed sample, C_A is the counting rate for the gold sample, C_{SA} is the corresponding carbon sample counting rate, N_A and N_X are the sample thicknesses of the gold and of the analyzed sample and ε_A and ε_X are the average spectrum fractions. Although "σ_γ" has the dimensions of a cross section, it should be noted that it is not identical to the true capture cross section, since it still contains the effects of resonance self-shielding, multiple scattering and resolution broadening. Furthermore, possible deviations of resonance pulse height spectra from the average pulse height spectrum and differences between the detector efficiencies for the measured sample and for gold are neglected. All these effects were taken into account in the next step of the calculations, the determination of radiation widths. For resonances with known spin and total width the radiation width can be found by shape or area analysis. In the present work detailed multi-level fits of the transmission of ^{47}Ti and ^{61}Ni had yielded spins and total widths (ref. [37]), and for ^{56}Fe, ^{58}Ni and ^{60}Ni

a few values were known from the literature (ref. [4]). Capture yield analysis was performed with a modified version of the program TACASI (ref. [5]). This program fits measured capture areas by adjusting the radiation widths. The TACASI code uses sums of single-level terms to represent the total cross section and the capture cross section. The effect of multiple scattering is calculated by Monte Carlo methods. Since the resonances investigated have usually much larger neutron width than radiation width, multiple interactions were important. The contribution of multiple interactions are listed in Table III.

6. RESULTS

Capture yields divided by the sample thicknesses are shown in Figures 1 - 7 and 9 - 21. Many resolved resonances can by seen in the capture yield. The number of resonances observed over a fixed neutron energy interval is given in Table II.

The calculations of radiation widths are not yet finished. The results obtained until now are given in Table III.

Pulse height spectra obtained from a natural iron sample are given in figure 8. Table 4 gives details on the spectra. The relative coincidence efficiency is the relative efficiency obtained with majority coincidence (at least two quarters of the scintillator tank must give a signal for a capture event to be recorded).

7. DISCUSSION

The main result of the present work are the capture cross sections presented in Figs. 1 - 7 and 9 - 21 and the radiation widths listed in Table III.

In several cases the isotopic assignments differ from those given in ref. [6], where essentially the same samples were used. An important improvement of the analysis methods applied in the present work over those of ref. [6] is the inclusion of well-analyzed total cross section data, especially resonance spins and neutron widths, in the analysis. This enabled us to extract a large number of radiation widths, particularly for most of the broad s-wave resonances. The only level where previously reported values could be compared to our numbers is the 27.9 keV resonance of ^{56}Fe+n. Our result, (1.4 ± 0.2) eV, agrees well with the published values (1.5 ± 0.3) eV [8], 1.3 eV [7] and (1.44 ± .14) eV [6]. The radiation widths for ^{60}Ni and ^{61}Ni are much larger (roughly 2 eV) than those of other nuclei with similar masses (roughly 0.5 eV, see ref. [9]). This seems to confirm conclusions reached by Moldauer [10] who had to assume radiation widths of the order of 1 eV for the nickel isotopes in order to fit unresolved capture data. Schmitt [11] estimated even higher radiation widths, using measured resonance integrals and thermal capture cross sections. Kuklin [12] gives a simple formula to estimate average radiation widths from the

nuclear mass, the effective excitation energy and the single-particle level density at the Fermi energy. With this formula one finds values between 1 and 2 eV, depending a little on the way in which pairing corrections are applied to the excitation energy and on the single-particle level densities chosen. The main effect, according to Kuklin's formula, comes from the rather small single-particle level densities and high binding energies of the nickel isotopes, which in turn are related to the magic proton number of nickel.

ACKNOWLEDGEMENT

We wish to acknowledge the cooperation of the USAEC and Euratom agencies and committees who helped us to get the enriched isotopic samples. We thank Professor Beckurts for his interest in this work. The help of the Van de Graaff crew is also appreciated.

REFERENCES

[1] Kompe, D., Nucl. Phys. A141 (1970) 602.

[2] Kompe, D., Ernst, A. and Fröhner, F.H., Nucl. Phys. A133 (1966) 513.

[3] Cho, M., et al., Total Cross Section of ^{45}Sc,..., Contribution to this Conference.

[4] BNL 325, Second Edition, Supplement No. 2, 1966.

[5] Fröhner, F.H., General Atomic Report GA-6906 (1965).

[6] Hockenbury, R.W., et al., Phys. Rev. 178 (1969) 17.

[7] Moxon, M.C., International Conference on the Study of Nuclear Structure with Neutrons, Antwerpen, 1965 (North Holland Publishing Co., Amsterdam, 1966).

[8] Macklin, R.L., Pasma, P.J. and Gibbons, J.H., Phys. Rev. 136 (1964) B695.

[9] Julien, J., et al., Nucl. Phys. A132 (1969) 129.

[10] Moldauer, P.A., Vienna Seminar on the Physics of Fast and Intermediate Reactors, 1961, Vol. 1, p. 171.

[11] Schmidt, J.J., Report KFK 120 (1966).

[12] Kuklin, R.N., Sov. J. Nucl. Phys. 7 (1968) 337.

TABLE I

Sample	Chemical Form	Total Weight (g)	Enrichment (%)	Thickness (10^{-3} nuclei/barn)
^{47}Ti	TiO_2	41.7	79.5	4.664
^{56}Fe	Fe_2O_3	71.5	99.7	9.924
^{58}Ni	Ni	55.0	99.9	10.567
^{60}Ni	Ni	55.0	99.8	10.215
^{61}Ni	Ni	27.4	91.8	4.598
^{197}Au	Au	120.3	100.0	5.782

TABLE II

Nuclide	Energy Interval (keV)	Number of Observed Resonances	Average Spacing (eV)
^{47}Ti	30	35	860
^{56}Fe	100	20	5000
^{58}Ni	100	33	3000
^{60}Ni	100	26	3800
^{61}Ni	30	38	790

TABLE III

Nuclide	Resonance Energy (keV)	Radiation Width (eV)	Multiple Scattering Contribution to Primary Capture Yield (%)
^{47}Ti	8.11	1.4 ± 0.3	5
	8.33	2.0 ± 0.4	27
	10.5	1.6 ± 0.2	3
	12.2	2.1 ± 0.5	6
	12.8	2.5 ± 0.5	5
	16.4	2.0 ± 0.4	11
	17.4	2.0 ± 0.3	1
	19.0	2.5 ± 0.5	1
	21.2	1.7 ± 0.3	1
	average :	1.81 ± 0.11	
^{56}Fe	27.8	1.4 ± 0.2	59
^{60}Ni	12.5	3.4 ± 0.7	159
	28.5	1.2 ± 0.4	54
	65.5	2.2 ± 0.3	5
^{61}Ni	7.16	2.5 ± 0.4	11
	7.55	2.3 ± 0.6	70
	8.75	2.6 ± 0.8	2
	12.6	1.7 ± 0.3	7
	13.6	1.6 ± 0.4	7
	14.0	3.1 ± 0.5	7
	16.7	2.2 ± 0.4	
	17.9	1.6 ± 0.5	10
	18.9	0.9 ± 0.3	12
	24.6	1.4 ± 0.3	2
	28.2	3.0 ± 1.0	1
	29.1	2.4 ± 0.4	25
	33.7	2.8 ± 0.5	1
	37.1	3.0 ± 0.5	1
	average :	1.94 ± 0.12	

TABLE IV

Figure 8 Spectrum No.	Resonance Energy (keV)	Isotopic Assignement	Relative Coincidence Efficiency
1	10.2	54	
2	13.9	57	
3	14.4	54	
4	22.8	56	0.84
5	27.7	56	0.66
6	30.5	54	
7	34.2	56	0.43
8	36.7	56	0.81
9	38.3	56	0.71
10	45.8	56	0.95
11	52	56	0.73
12	53	56	0.94
13	59	56	0.60
14	63	56	1.00
15	73	56	0.45
16	77	56 + 54	
17	81	56	0.80
18	83	56	
19	90	56	
20	93	56	
21	96	56	
22	102	56	0.70
23	105	56	0.44
24	112	56	
25	129	56	

FIGURE CAPTIONS

Fig. 1 - 5 ^{47}Ti capture yield divided by sample thickness versus energy; triangles: low energy run, circles: high energy run.

Fig. 6 - 7 ^{56}Fe capture yield divided by sample thickness versus energy; triangles: low energy run, circles: high energy run.

Fig. 8 Natural iron. Pulse height spectra of individual resonances. See table IV.

Fig. 9 - 12 ^{58}Ni capture yield divided by sample thickness versus energy; triangles: low energy run, circles: high energy run.

Fig. 13 - 16 ^{60}Ni capture yield divided by sample thickness versus energy; triangles: low energy run, circles: high energy run.

Fig. 17 - 21 ^{61}Ni capture yield divided by sample thickness versus energy; triangles: low energy run, circles: high energy run.

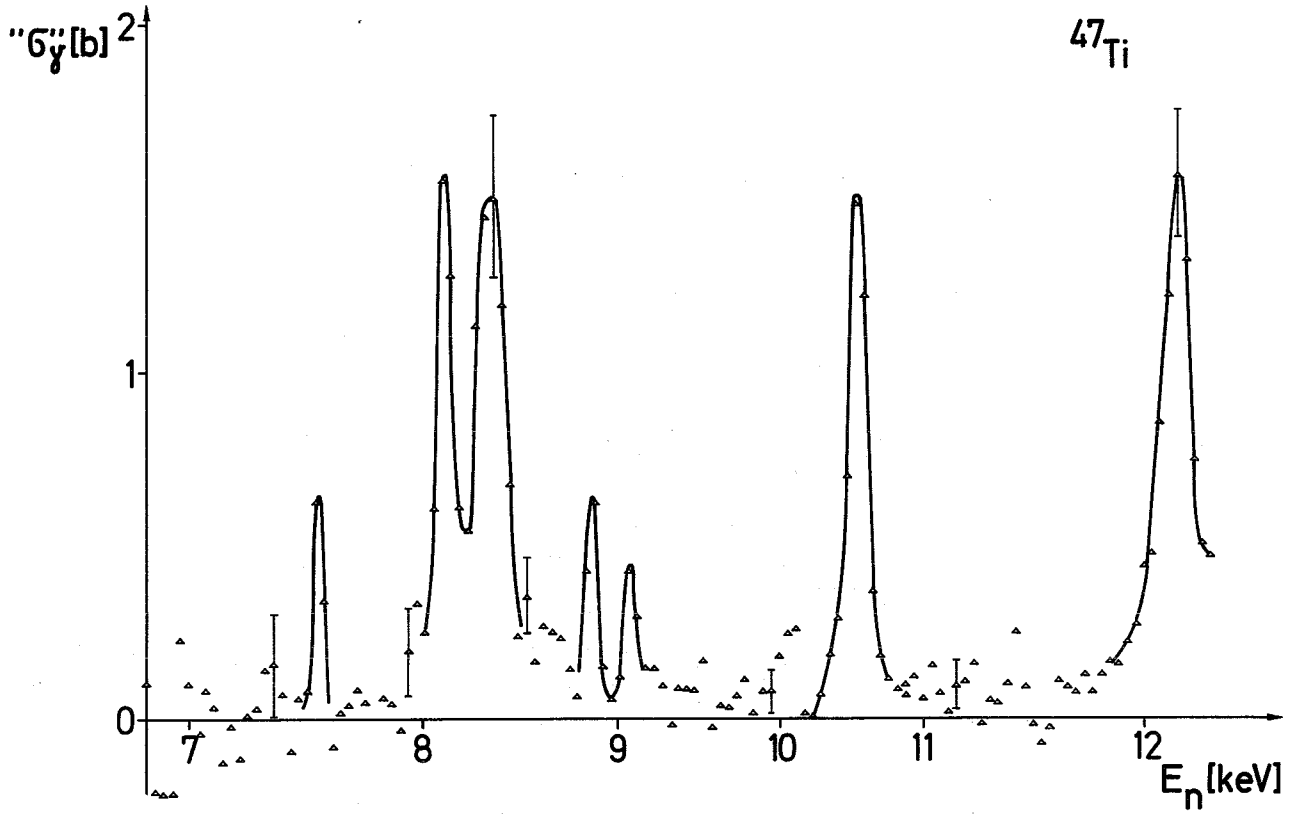

Figure 1

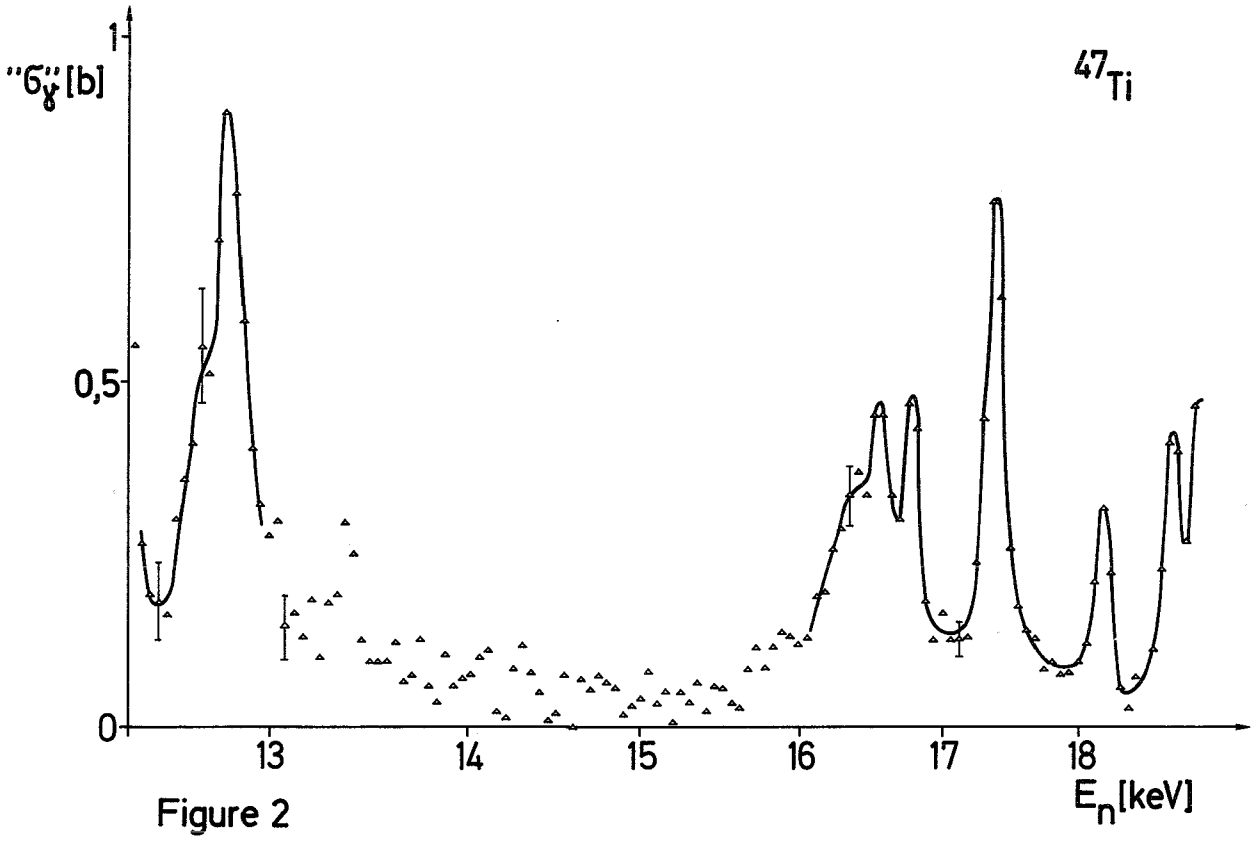

Figure 2

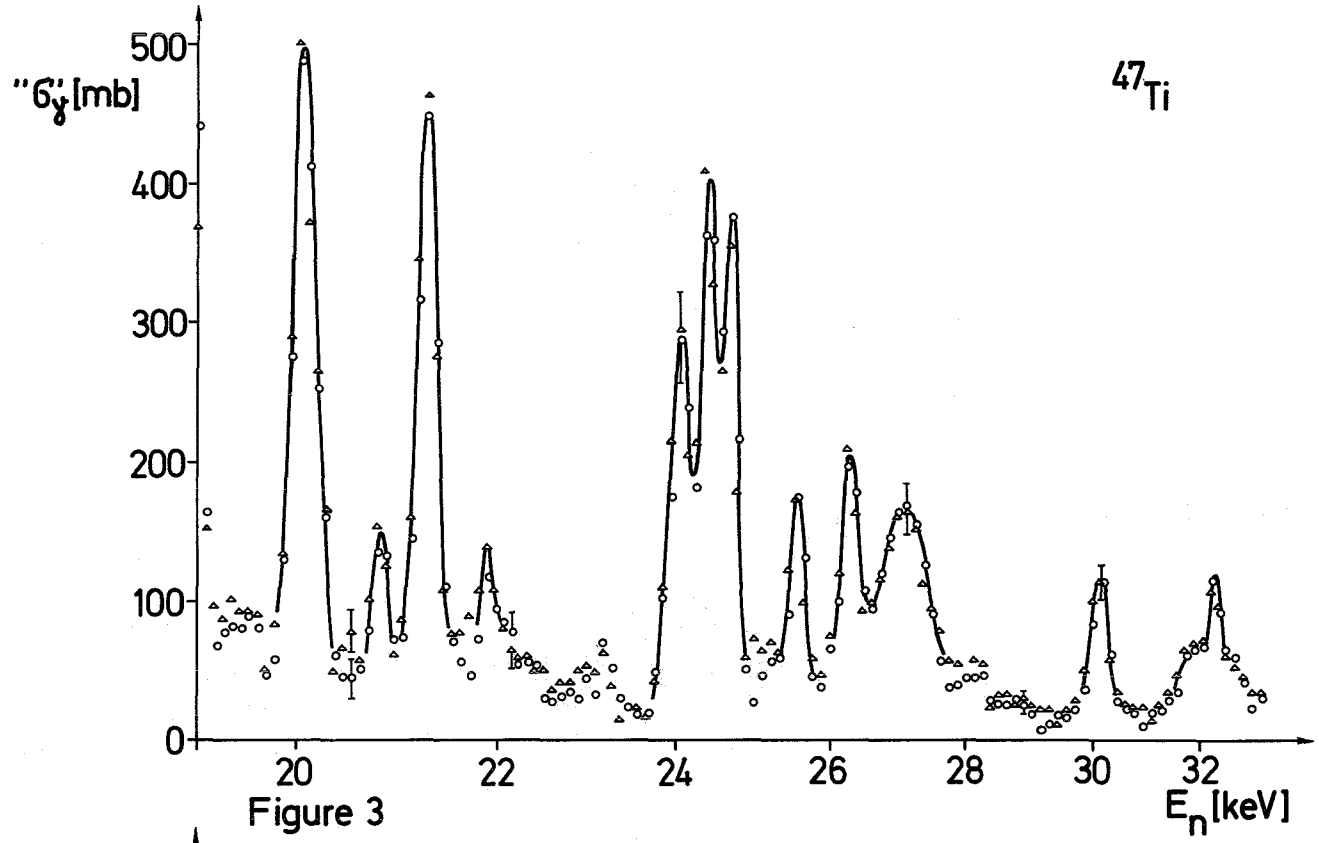

Figure 3

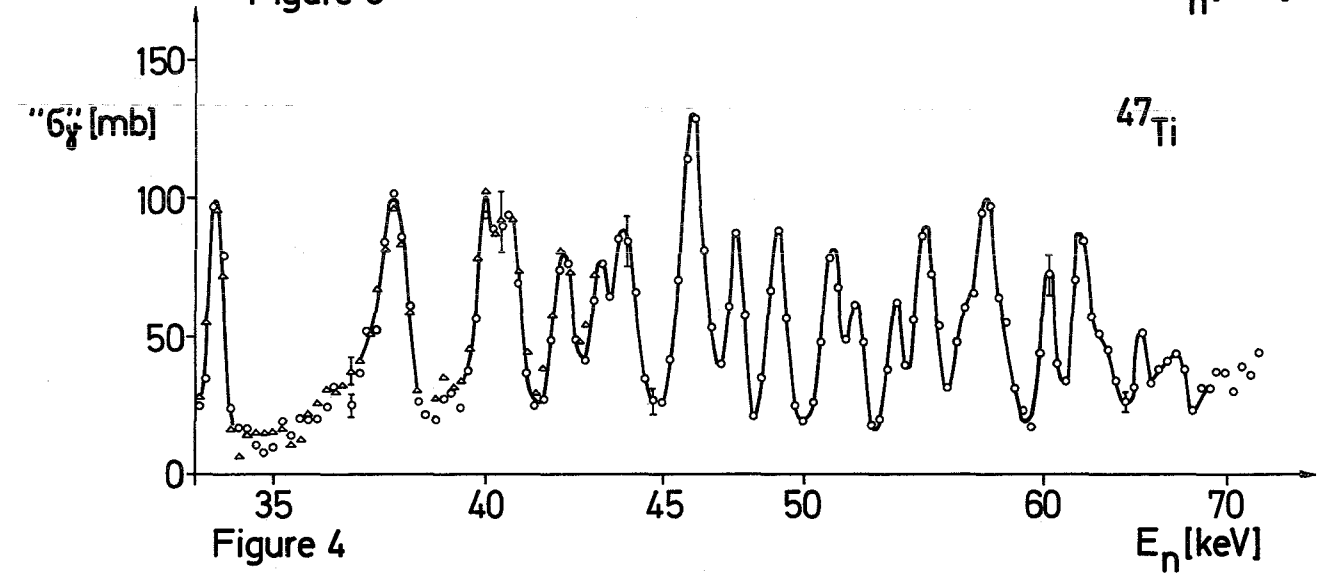

Figure 4

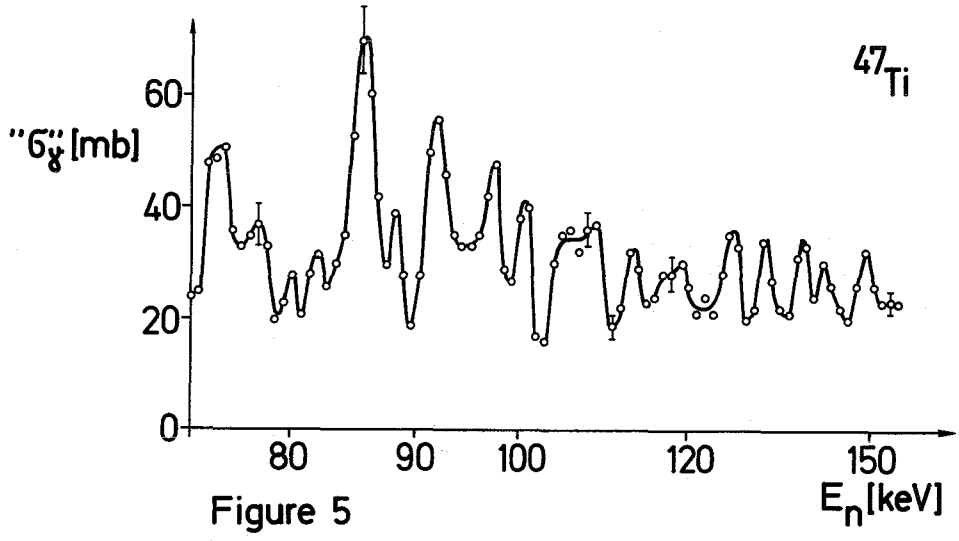

Figure 5

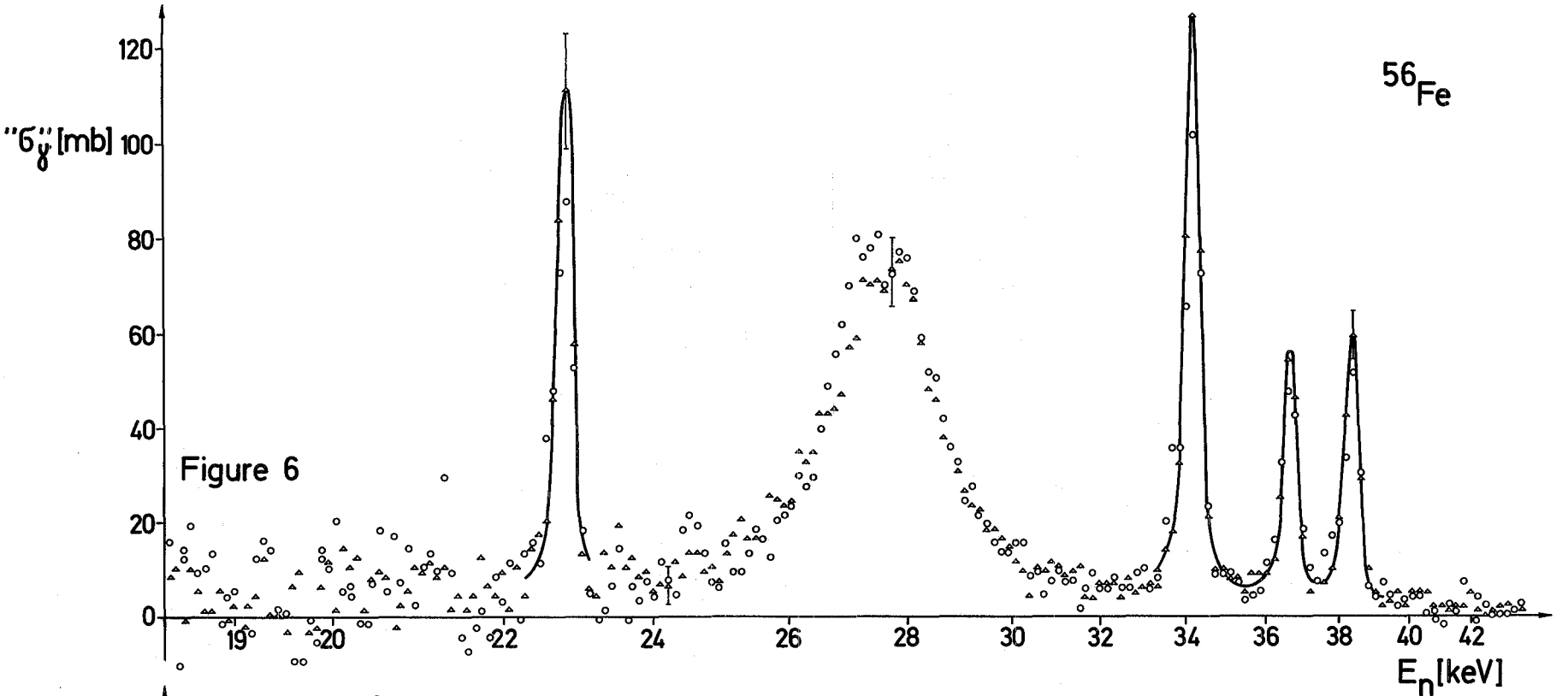

Figure 6

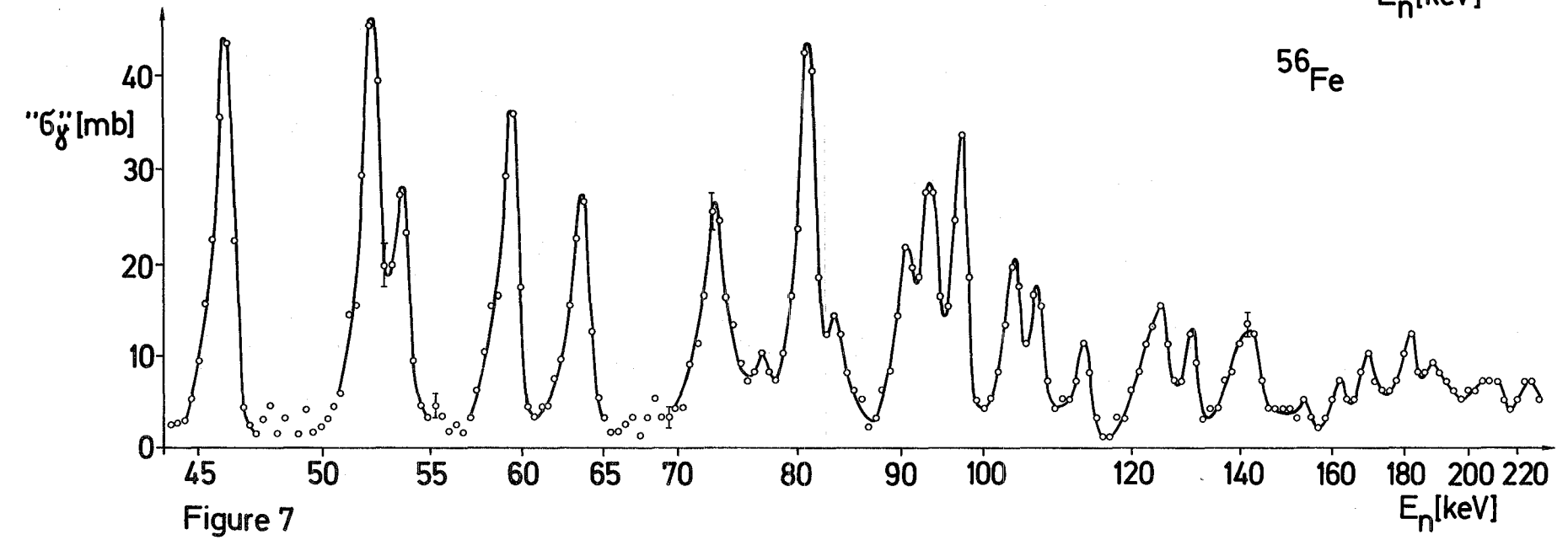

Figure 7

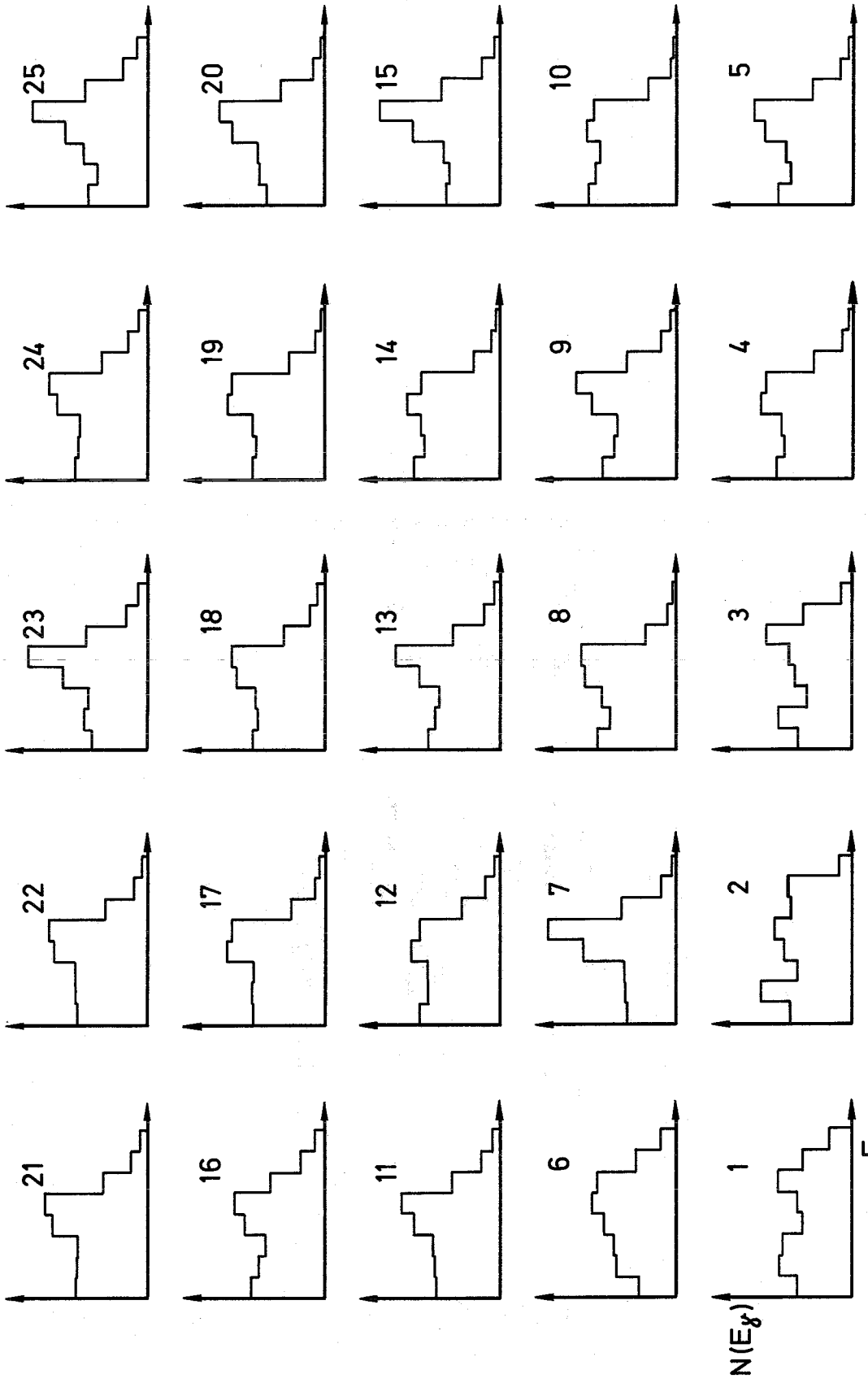

Figure 8

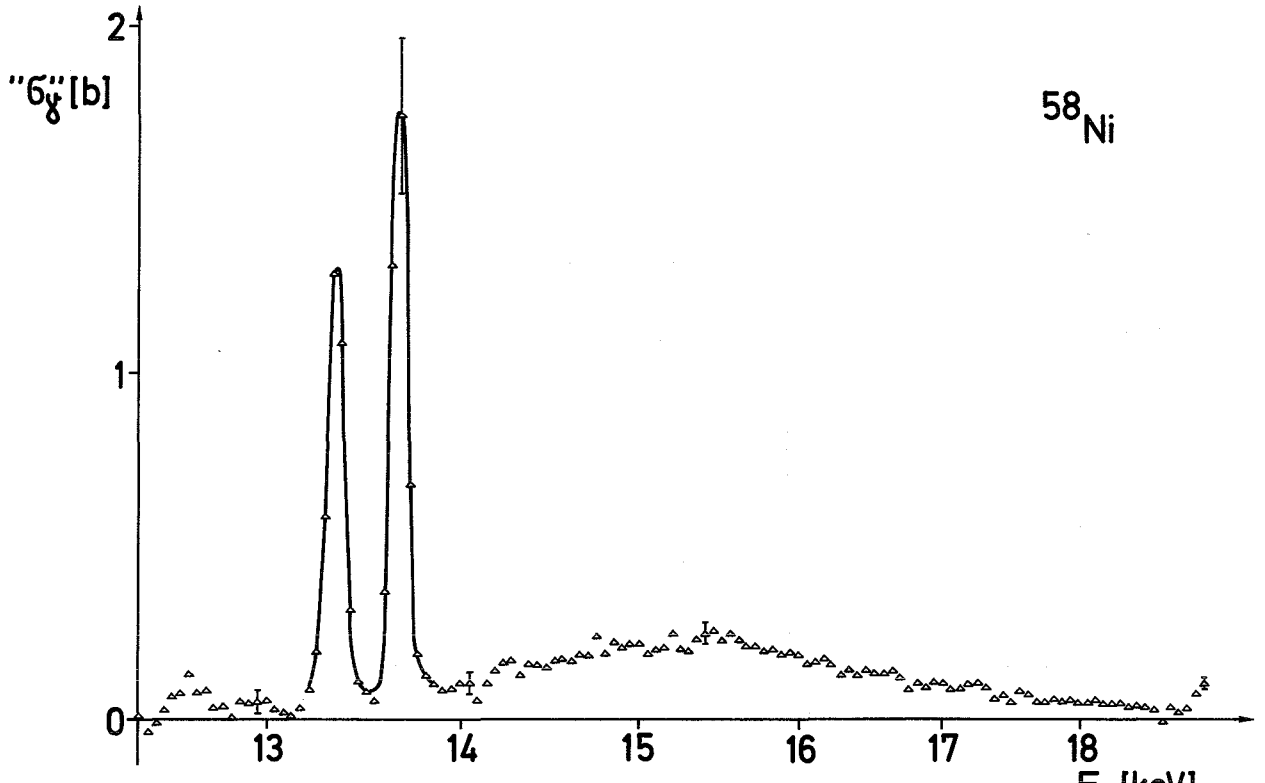

Figure 9

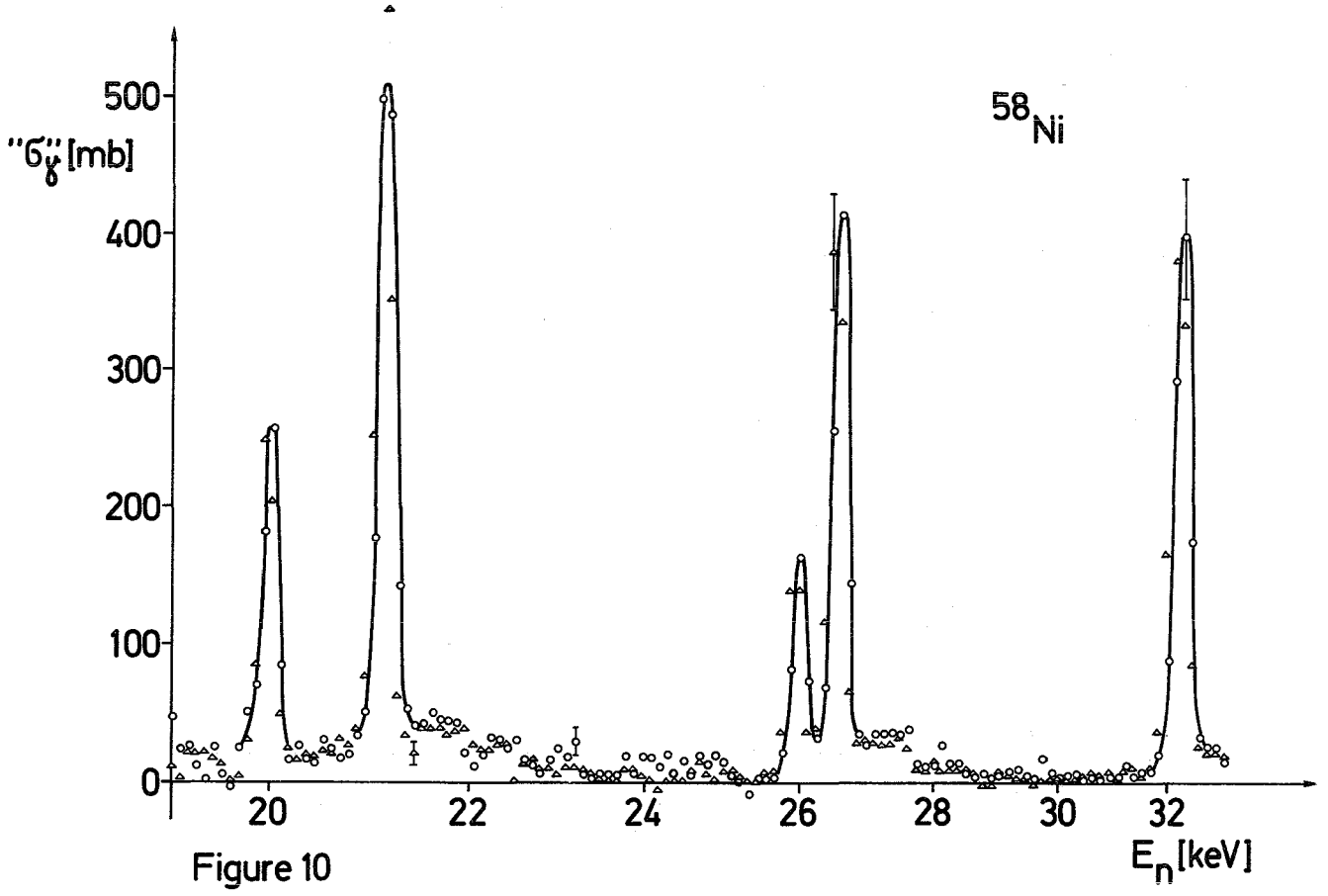

Figure 10

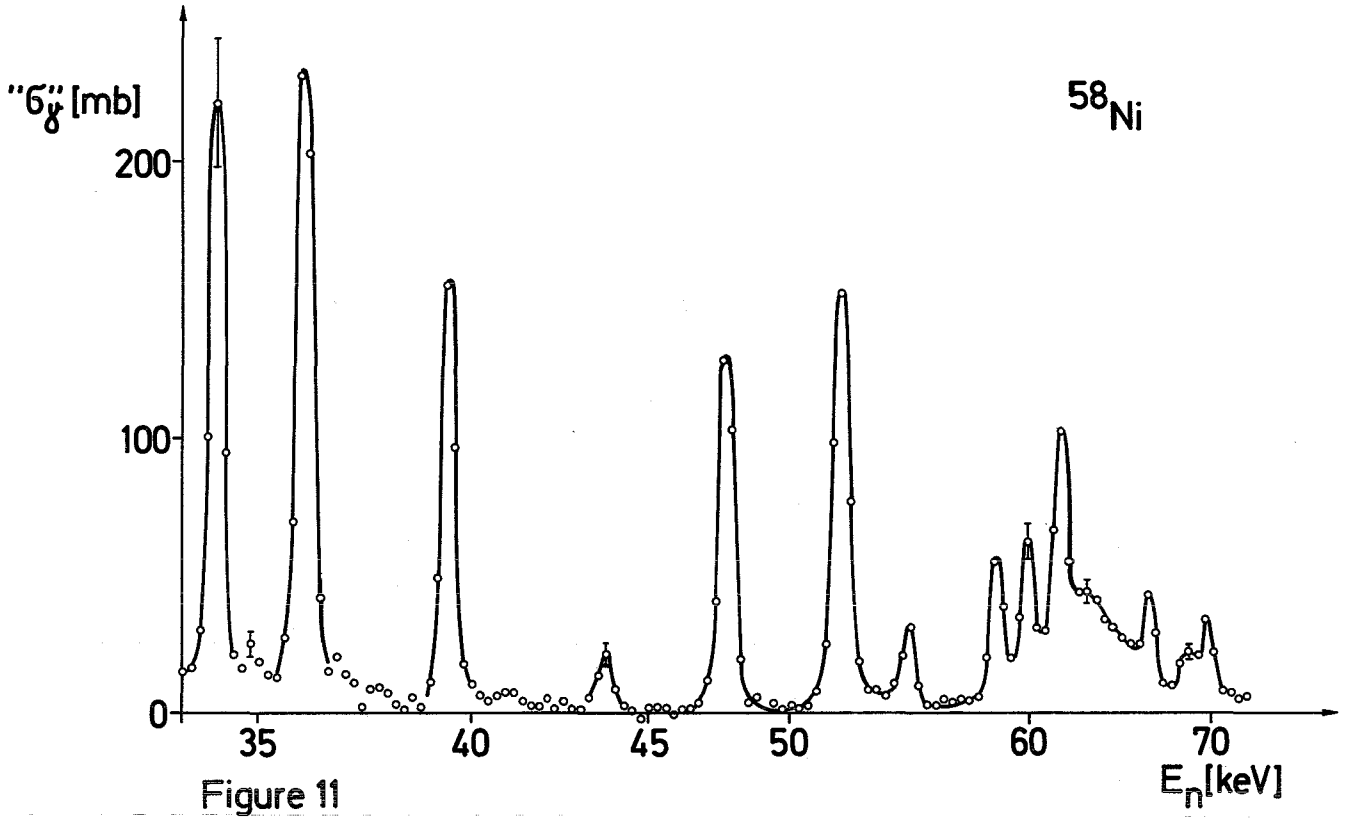

Figure 11

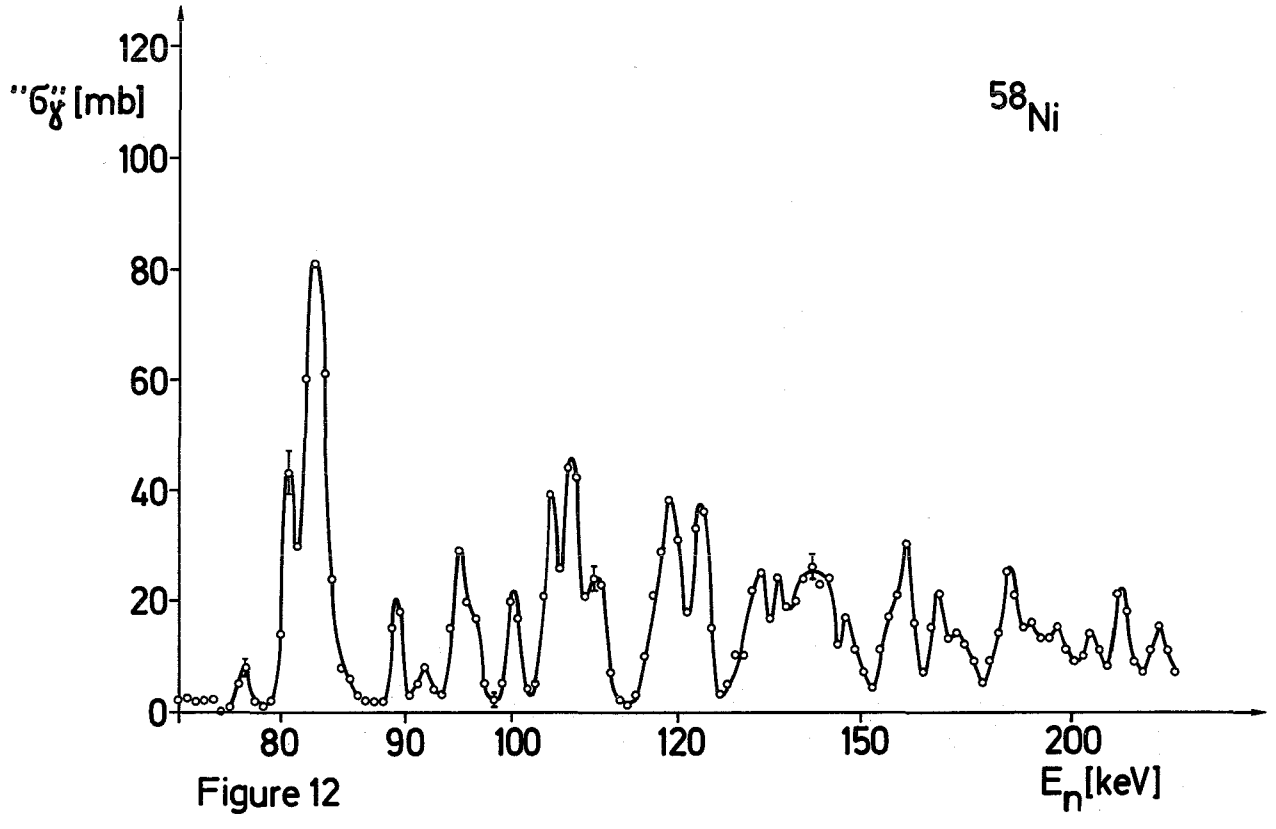

Figure 12

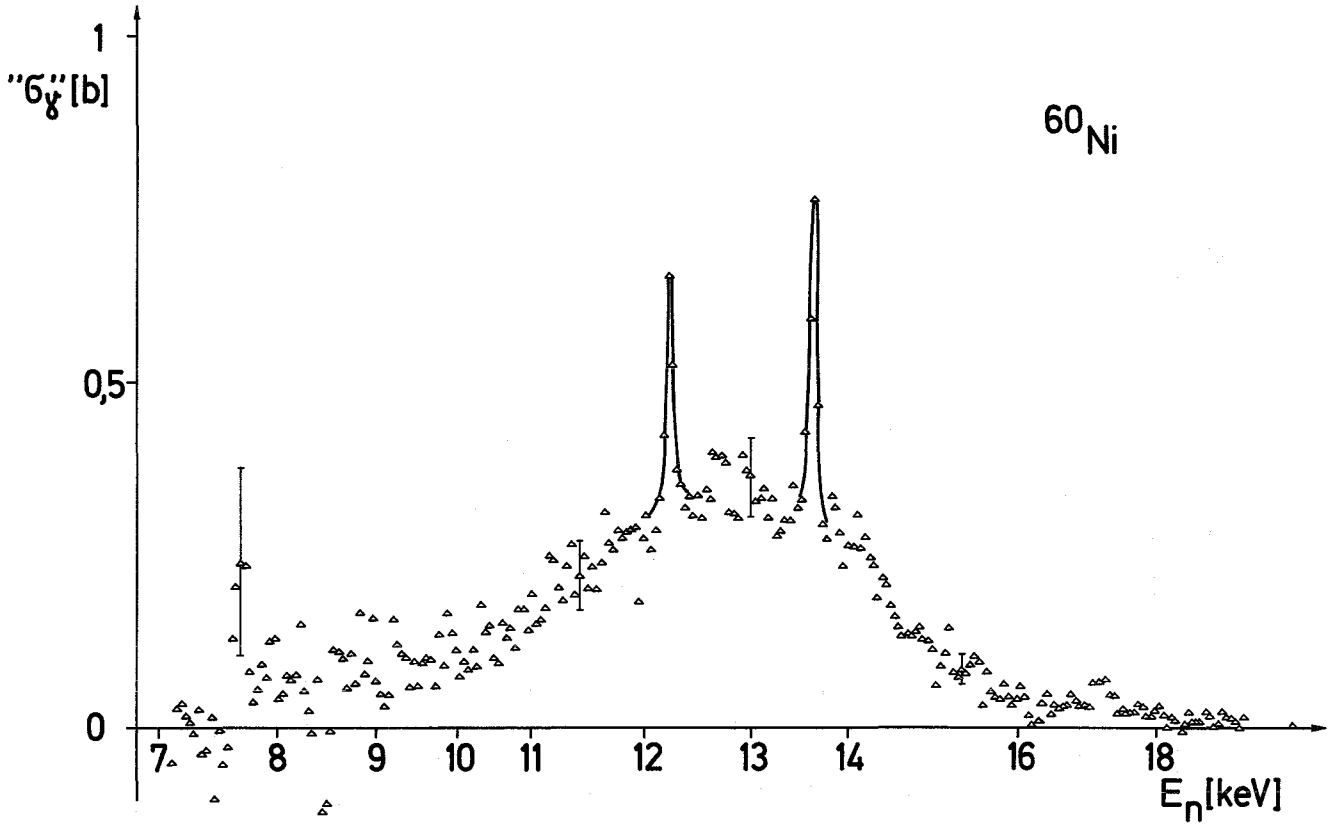

Figure 13

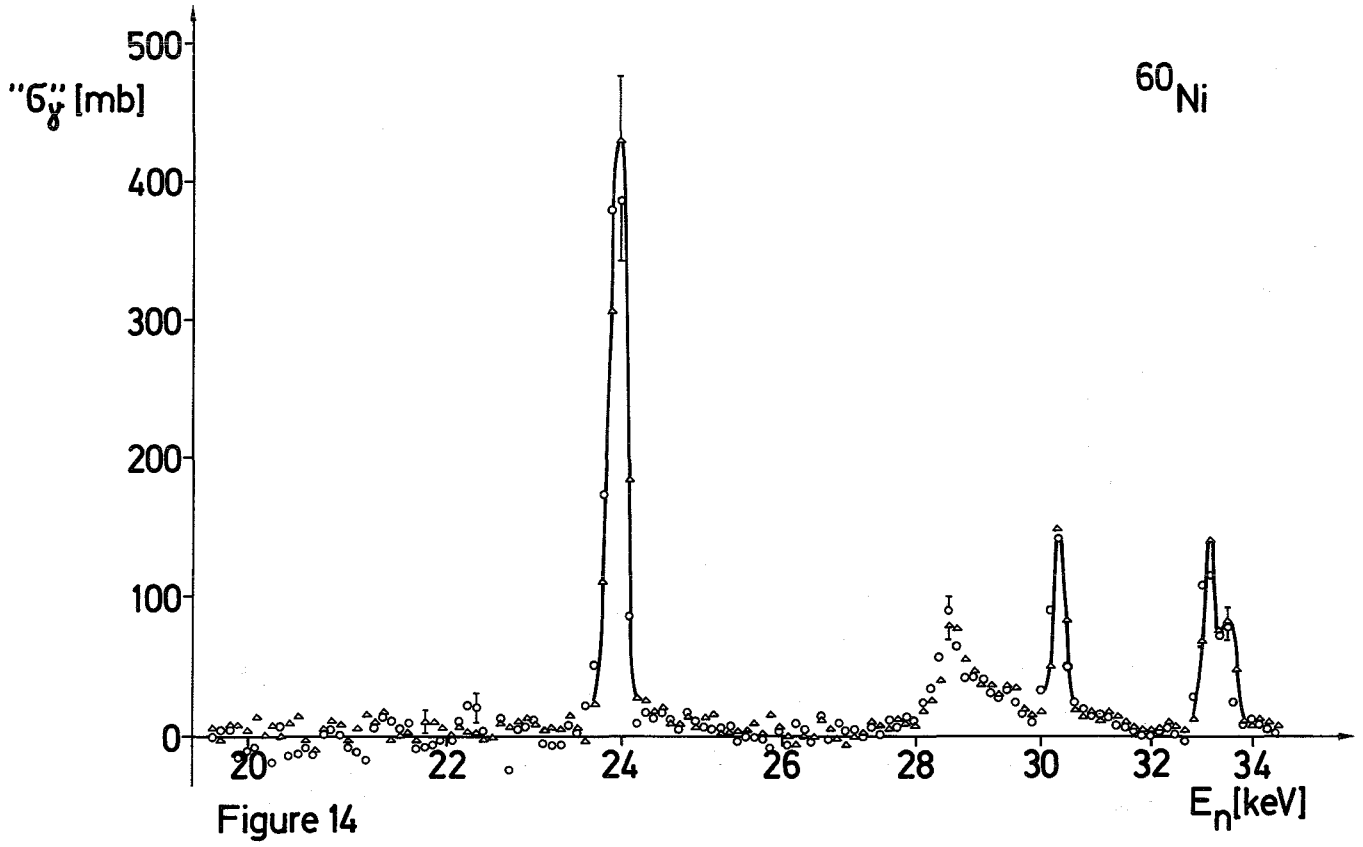

Figure 14

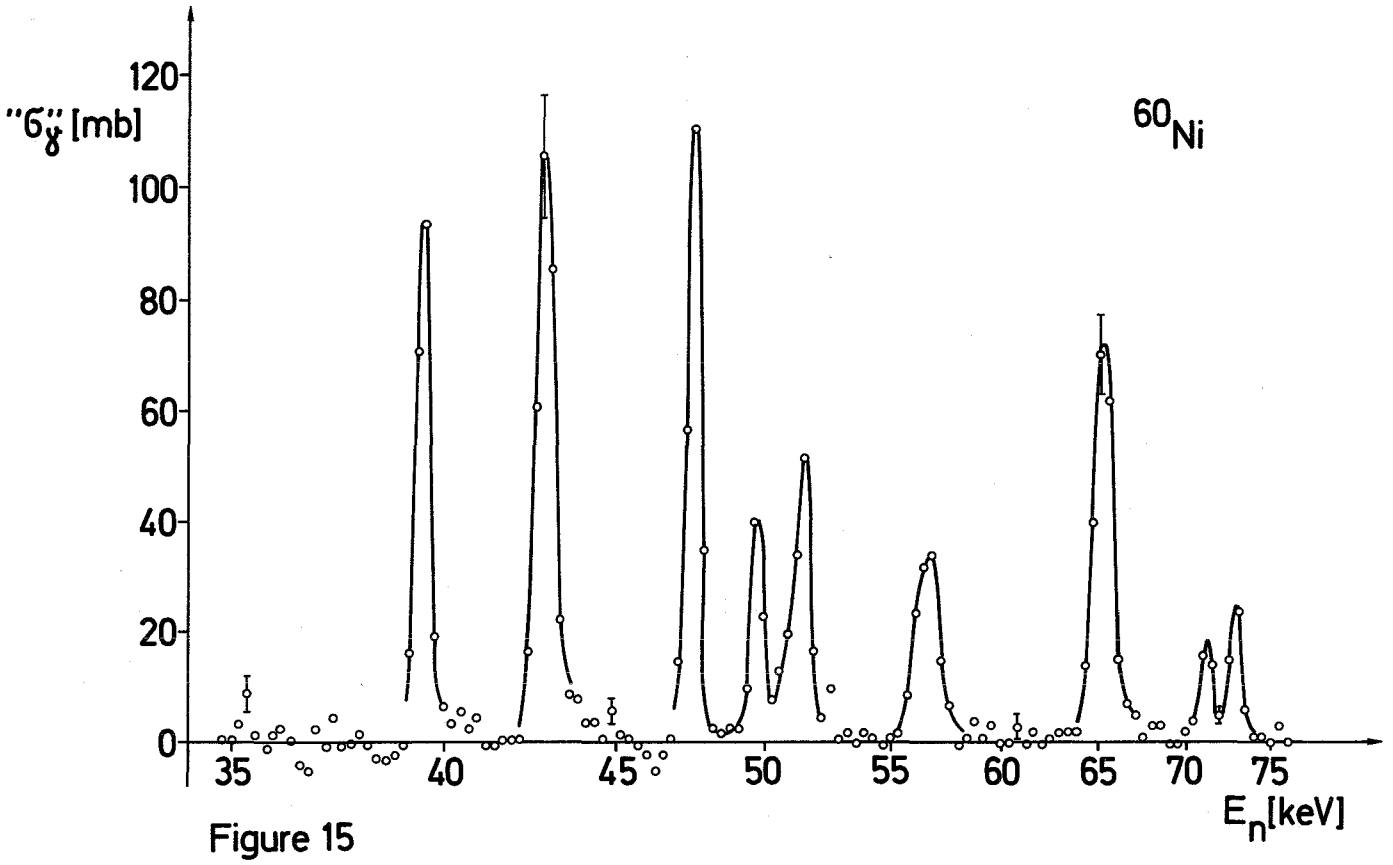

Figure 15

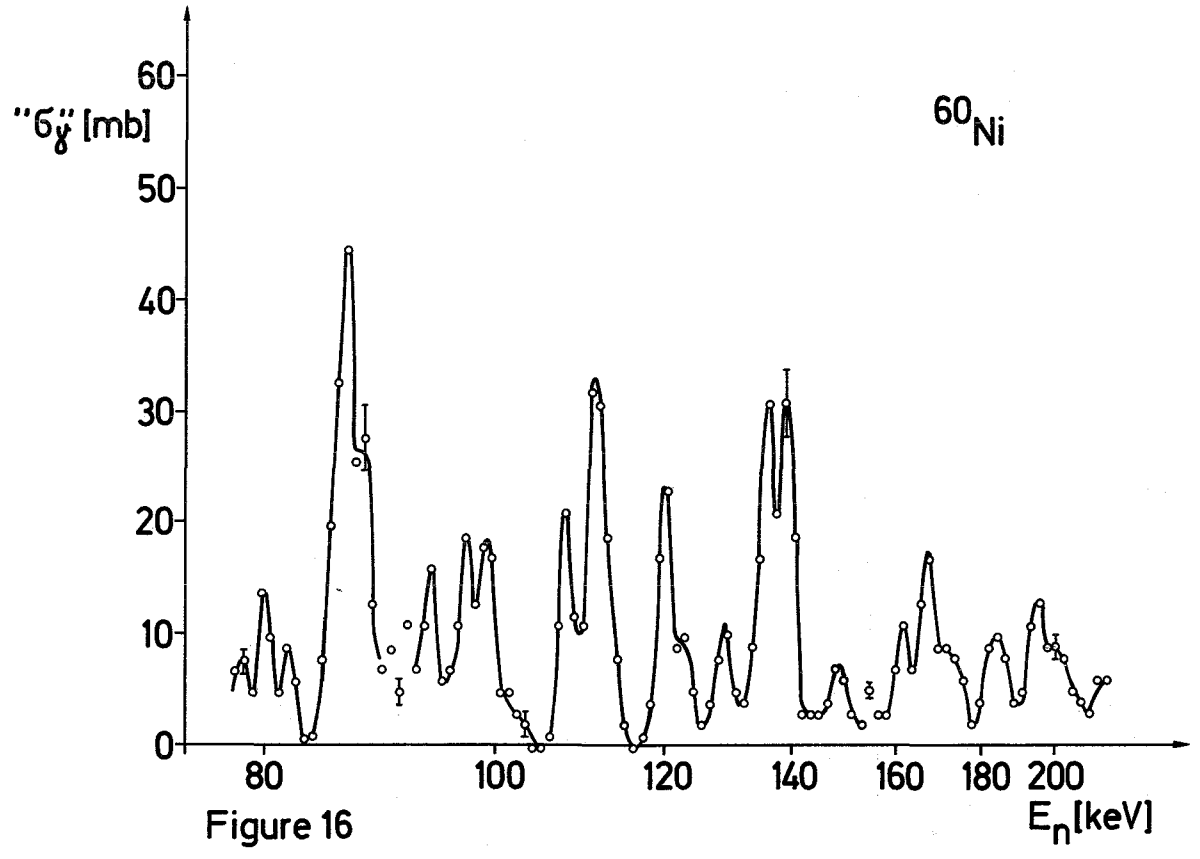

Figure 16

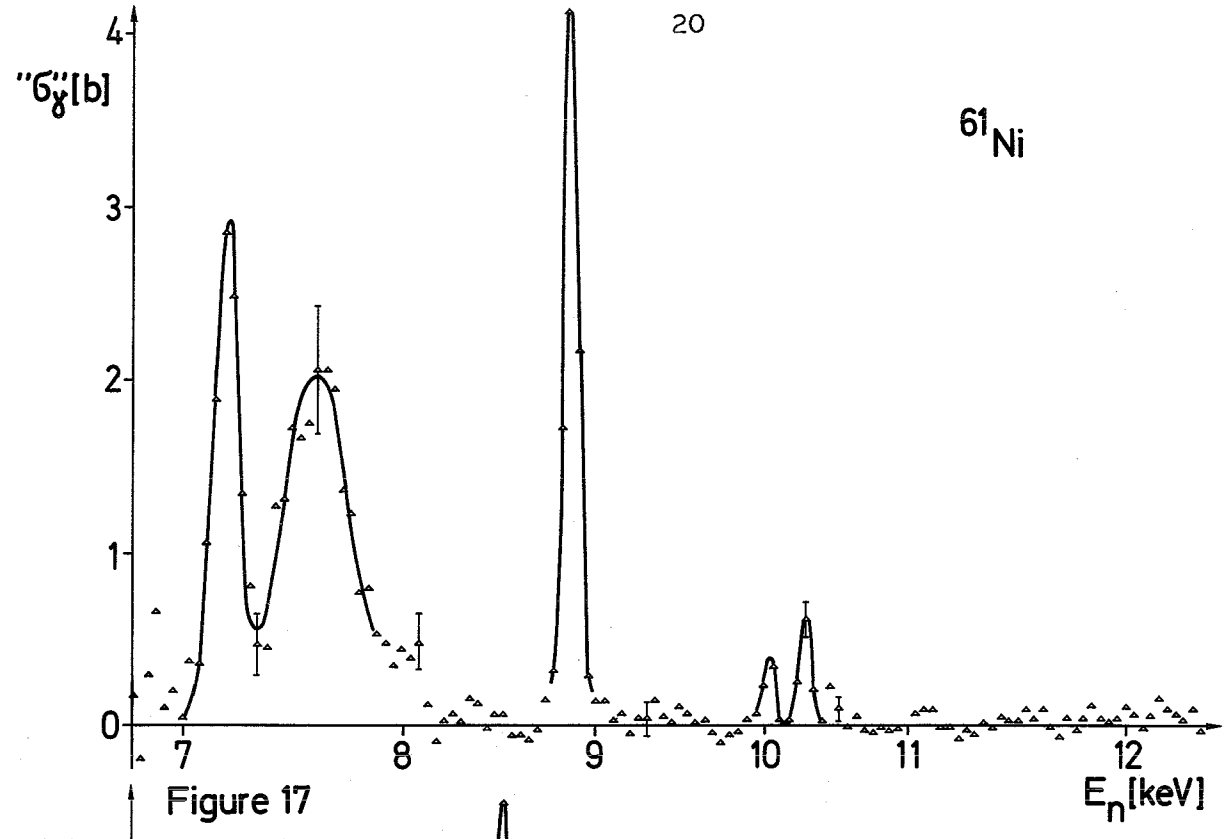

Figure 17

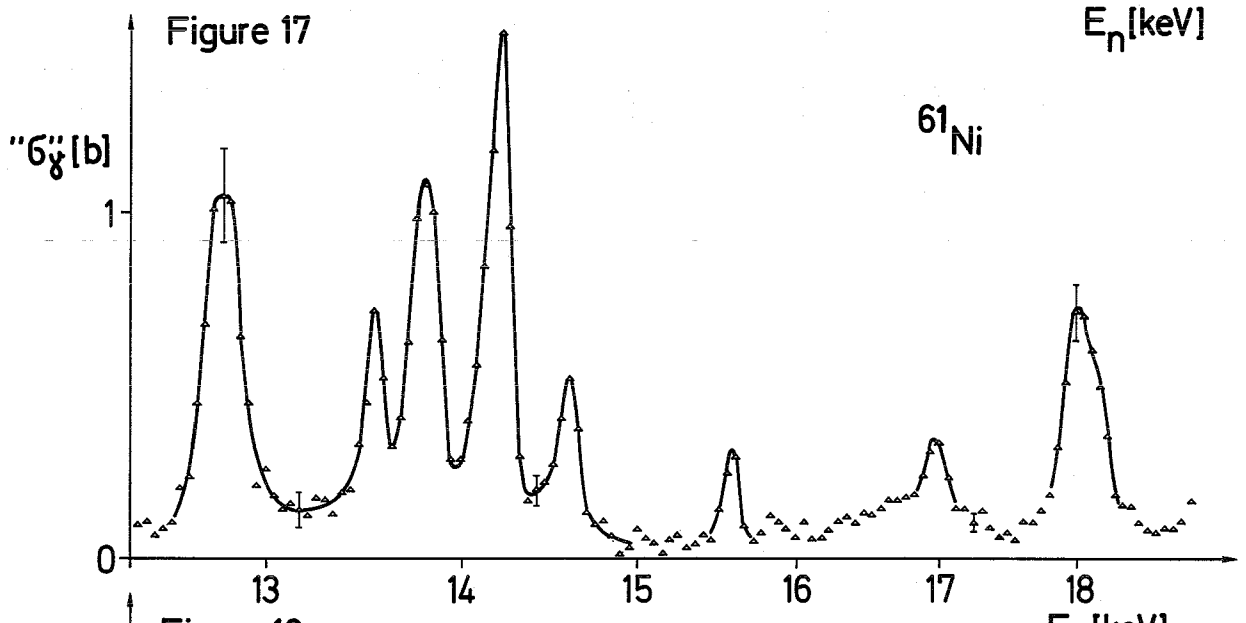

Figure 18

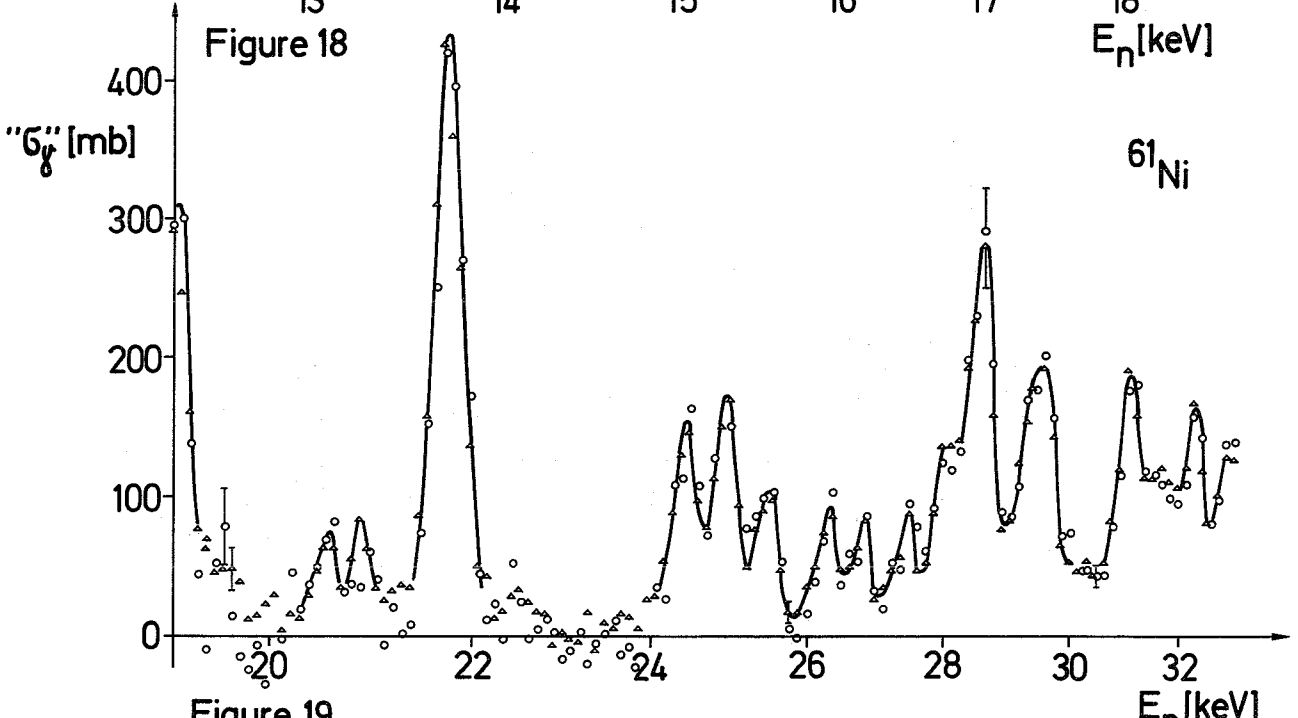

Figure 19

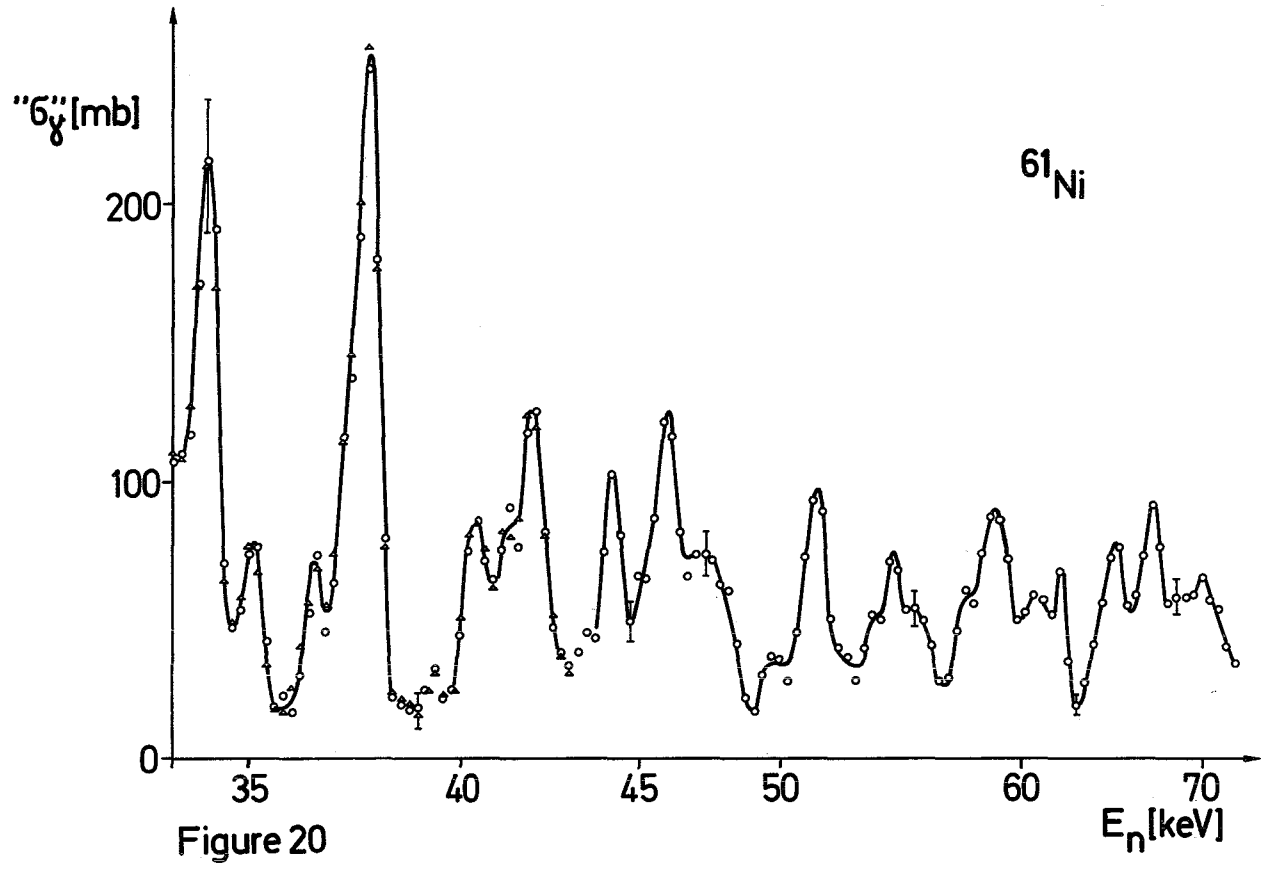

Figure 20

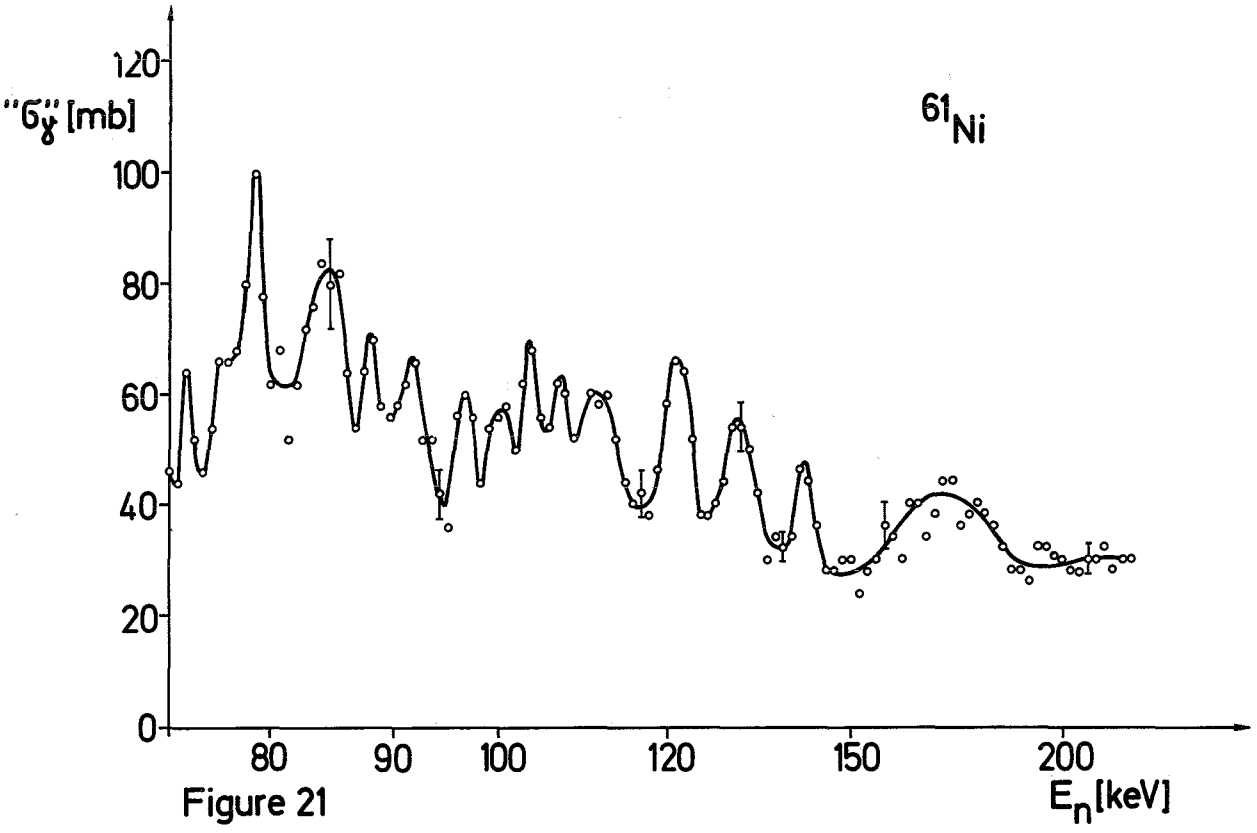

Figure 21